Pérez Zapata, K.; Lenis, J.; Rico Tortosa, PM.; Gómez Ribelles, JL.; Bolívar, F. (2022). Determination of synergistic effect between roughness and surface chemistry on cell adhesion of a multilayer Si- Hydroxyapatite coating on Ti6Al4V obtained by magnetron sputtering. Thin Solid Films. 760:1-8. https://doi.org/10.1016/j.tsf.2022.139489

Determination of synergistic effect between roughness and surface chemistry on cell adhesion of a multilayer HA-Si coating on Ti6Al4V obtained by magnetron sputtering.

K. Pérez [a], J.A. Lenis *[a,b], P. Rico [c,d], J.L Gómez Ribelles [c,d], F.J. Bolívar [a]

[a] Centro de Investigación, innovación y Desarrollo de Materiales CIDEMAT, facultad de ingeniería, Universidad de Antioquia, Medellín, Colombia.

[b] Centro de Formación Minero Ambiental, Servicio Nacional de Aprendizaje (SENA), Colombia.

[c] Centre for Biomaterials and Tissue Engineering (CBIT), Universitat Politècnica de València, Valencia 46022, Spain.

[d] Biomedical Research Networking Center on Bioengineering, Biomaterials and Nanomedicine (CIBER-BBN), Spain.

***Corresponding author: J.A. Lenis** julian.lenis@udea.edu.co

Abstract

Ti alloys are widely used in the biomedical field because they have an adequate balance between mechanical properties, corrosion resistance and biocompatibility. However, when this material is implanted in the human body, unfavorable reactions may appear that prevent

arise a good osseointegration due to the formation of a fibrous and non-adherent layer between the biomaterial and the bone, which can lead to failure or rejection of the implant. In this study, the influence of surface modification of Ti6Al4V alloy with a hydroxyapatite (HA) and silicon (Si) coating on its biological response in vitro was evaluated. The deposition process was performed by sputtering on two Ti6Al4V surfaces, Ti6Al4V - G and Ti6Al4V - R with different root mean square roughness values, the first one with 3.8 nm and the second one with 48.7 nm. The surface morphology of the coatings was observed by Scanning Electron Microscopy and Atomic Force Microscopy, the chemical composition was evaluated by X-ray Energy Dispersive Spectrometry and micro-Raman Spectroscopy. The in vitro biological response of the coatings was evaluated by MTT assay and cell adhesion tests, using mouse mesenchymal stem cells. The control of the process parameters allowed obtaining coatings with good compositional balance (Ca/P ratio very close to 1.67 and characteristic vibrations of the HA phase). Roughness values of 27 ± 5 nm and 52 ± 6 nm were obtained for the multilayer coatings obtained on Ti6Al4V - G and Ti6Al4V - R, respectively. Biological assays indicated a potentially non-toxic character of the coatings, moreover, the cell adhesion of Ti6Al4V was favored both by the incorporation of the HA-Si multilayer coating and by the increase in the roughness of the substrate.

Keywords: hydroxyapatite, silicon, sputtering, structure, cell viability.

1. Introduction

Magnetron sputtering (MS) is a synthesis process by which stoichiometric coatings can be obtained [1]. The production of coatings is carried out inside a high-vacuum chamber, where

a reactive or non-reactive plasma is created, which allows the transport of the species that travel from a target and are deposited on a substrate [2]. MS allows the production of coatings with thicknesses of less than 1µm, providing them with uniformity, density, and good adhesion on substrates of different nature, whether ceramic, polymeric or metallic [3]. Metallic materials, especially some titanium (Ti)-based alloys are the most common for biomedical purposes, because they are considered bioinert materials in the human body [4]; some of the characteristics of Ti alloys are low density, high strength, non-toxicity and good corrosion resistance [5], which makes them suitable for use in orthopedic and dental implant applications. Not only these characteristics have caught the attention on these alloys, but also their high performance in mechanical resistance, which have motivated the development of corrosion-fatigue studies, since most implants are subjected to dynamic loads in corrosive media [6]. However, some cases have been reported on inflammatory reactions around implants, resulting from the formation of avascular fibrous tissue due to lack of osseointegration of the implanted device [7]. To solve this, materials such as calcium phosphates have been used, in particular hydroxyapatite (HA) [8], being the inorganic mineral present in bones and teeth [9]. HA exhibits important properties as biomaterial, such as osteoconduction and biocompatibility. Thanks to the characteristics presented by HA, various biomaterials have been developed that have expanded the diversity of its applications [10], which has shown significant success with in vivo and in vitro behavior [11]. Although there is evidence of bone growth on the HA surface after the implantation process, its beneficial effect as a bioactive material in osseointegration can still be enhanced [12], [13]. The biofunctionality and bioactivity of HA depend on its structure, composition and morphology; likewise, it has been reported that the presence of bioactive elements such as F, Mg, Zn, Sr, Ag and Si can improve biological performance and cell behavior [11], [14], [15].

An approach to improve HA osseointegration is to dope it with some beneficial elements that are present in human bone [16]. As it is well known, silicon (Si) is an essential element in the metabolism and formation of hard tissues (in vitro). This is why it is suggested that doping HA with Si increases in performance for bone formation and calcification. It has been shown that the presence of Si increases the bioactivity of HA in vitro and in vivo [17]. Recently, it has been reported that HA with Si shows a high dissolution rate, suggesting a higher solubility, and, therefore, a higher biocompatibility [18] (production of high). Investigations in animal models revealed higher levels of bone apposition, ingrowth and adaptive remodeling [19], which has led to improvements in cell dispersion of HA coatings with Si [20], consequently, these systems improve the bond between the implant and the natural bone, in addition to being a nanoscale biomaterial with a high promotion of cell adhesion [21]. The surface properties of biomaterials such as hydrophobicity, hydrophilicity, roughness, surface electric charge and chemical composition are of great importance in cell adhesion and cell proliferation [22]. Surface characteristics can mediate the interaction by enhancing or affecting tissue integration after biomaterial implantation [23]. Several authors [24]–[26] have proposed models that establish that surface wettability is modified by surface roughness. To promote bioactivation, strategies for surface modification by varying the roughness of the substrates have been applied. In this work, the characteristics of HA-Si layers deposited on Ti6Al4V by magnetron sputtering are reported, in order to study the effect on the chemical composition, structure, cytotoxicity and cell adhesion, when the roughness conditions of the substrate are varied.

2. Experimental details

2.1. Coating development

Ti6Al4V disks with dimensions of 8 × 8 × 3 mm^3 were used as substrates. These were subjected to mechanical polishing, obtaining two types of samples: for the first one, corresponding to Ti6Al4V (G), silicon carbide paper # 100, 240, 320, 600, 1000, 1500 and 2000 was used. Subsequently, a polishing with 0.3 μm diamond paste was carried out until a mirror-type surface finish was obtained. For the second sample, corresponding to Ti6Al4V (R), the polishing process was interrupted on silicon carbide paper # 600. To free the substrates from all kinds of dirt and grease, an ultrasonic bath was used, so that they were immersed in a 1:1 acetone-ethanol solution for 15 minutes. The chemical composition of the substrate was evaluated by X-ray fluorescence using a Thermo ARL Optim'X WDXRF.

Before starting the deposition process, the chamber was brought up to a pressure of 0.05 Pa (background) and an ionic cleaning of the substrates was performed with argon using a voltage of -700 V for 30 min. To obtain the coatings, the following were used: a radio frequency source (RF) (13. 56 MHz, SEREM) and a direct current source (DC) (ADL, MARIS); 2 targets, the HA one with a purity of 99.99% and a Ca/P ratio of 1.67, and a Si one with a purity of 99.99%, each with dimensions of 500 × 100 × 3 mm^3. The HA-Si multilayers were deposited by applying an RF power of 600W to the HA target and a DC power of 90W to the Si target. The coatings were deposited in an argon atmosphere at 230°C and 0.5 Pa. An architecture composed of 5 HA layers deposited for 300 min and 4 Si interlayers deposited for 12 min was designed [27]. The structural configuration of the coating is schematically shown in Fig. 1.

Fig. 1. Structural coating scheme.

2.2. Chemical composition of the coatings

Micro-Raman spectroscopy was used to identify the characteristic vibrations of the functional groups, the analysis was performed with two scans, one of them between 200 cm-1 and 1200 cm-1, and the other scan was performed between 3400 cm^{-1} and 3800 cm^{-1} using a 750 nm He-Ne laser. Elemental analysis was performed in triplicate by energy dispersive X-ray spectroscopy using a Jeol instrument (JMS-6490LVTM, 20 kV).

2.3. Structure and roughness of the coatings

In order to observe the HA-Si multilayers formed, a ductile fracture was performed on the sample and the SEM technique was used to observe its cross section using the Jeol equipment described above, additionally, a $5 \times 5 \times 2$ μm^3 cut was performed on the surface of the coating by focused ion beam (FIB) technique using a ZEISS ARUGA Compact dual beam system, 30 kV, 500 pA, which allowed revealing the structure of the coating, which was observed by field emission scanning electron microscopy (FESEM) with a ZEISS Gemini-SEM500 equipment operated at 2 kV. The roughness of substrates and coatings was evaluated in

triplicate by atomic force microscopy (AFM) in a 5 × 5 μm^2 area, using Bruker Multimode 8 equipment.

2.4. *In vitro* cell viability

For this assay, mouse mesenchymal stem cells (mMSCs) were cultured in DMEM (Dulbecco's Modified Eagle) cell culture medium at 37°C with 5% CO_2 controlled atmosphere for approximately 8 days until confluence was reached. Cell viability was assessed in non-contact mode at 72 h by MTT (3-(4,5 dimethylthiazol-2-yl)-2,5-diphenyl tetrazolium bromide) assay (Roche), using a seed density of 10000 cells/cm² and following the methodology described in [28]. A Perkin Elmer Victor3 microplate reader spectrophotometer was used for absorbance measurements at 570 nm. The assays were performed in triplicate.

2.5. *In vitro* cell adhesion

The adhesion of the mMSCs on the surface of the coatings and the substrate was evaluated at 3 and 24 h. A density of 5000 cells/cm² was seeded on the surface of the materials in DMEM medium at 37°C and 5% CO_2. Cells were processed according to [29] using the antibodies described in Table 1 to achieve staining of focal adhesions, actin cytoskeleton and cell nucleus. Upon completion of the assay, the samples were observed on a Nikon Eclipse 80i fluorescence microscope.

Table 1. Antibodies used for cell adhesion assay.

Staining	***Primary antibody***	***Secondary antibody***
Focal adhesions and actin cytoskeleton	Antivinculin (Sigma), 1:400	Alexa Fluor 555 α-mouse (Invitrogen) 1:700, Alexa Fluor 488 Phalloidin (Invitrogen) 1:100.
Nucleus	DAPI (Vector laboratories) contained in Vectashield	---

2.6. Image analysis

Once the images were acquired at X40 magnification for the cell adhesion assay (n=20). These images were processed using Image J analysis software, which allowed us to make binary masks of the mMSCs adhered to the surfaces evaluated and to calculate the circularity, cell area, focal adhesion areas and focal adhesion number.

2.7. Statistical analysis

The results of the cell viability and adhesion assay were analyzed by analysis of variance using GraphPad Prims 6 XML software.

3. Results and discussion

3.1. Chemical composition

Table 2 presents the chemical composition of the substrate used, which corresponds to the commercial Ti6Al4V alloy. The multilayer coatings deposited on that substrate presented an atomic Ca/P ratio of 1.66, very close to the stoichiometric value of HA (1.67) [30]. This ratio is a distinctive feature for this calcium phosphate, and it helps to differentiate it from other apatites of different molecular formula and therefore, properties and characteristics such as solubility, pH and stability in biological media that yield lower bioactivity than HA [31]. Furthermore, the atomic percentage of silicon was 1.73%. The control of the amount of Si in this type of coatings is very important. It has been reported that HA coatings doped with Si amounts higher than 4.6% atomic generate a decrease in the mechanical performance of the system [32]. All the above evidence an effective control in the deposition parameters of the HA-Si coating.

Tabla 2. Chemical composition of the Ti6Al4V substrate.

	Element (% w/w)								
Sample	**Si**	**Ni**	**Mo**	**Fe**	**Ti**	**Al**	**V**	**W**	**Cu**
Ti-6Al-4V	0.031	0.191	0.013	0.068	90.26	5.02	4.49	0.079	0.023

The Micro-Raman spectra obtained for the HA-Si coating compared to the spectrum of a pure HA target are reported in Fig.2. The vibrational bands observed in Fig.2a for both

samples are associated with the phosphate anion $(PO_4)^{-3}$ present in the molecular structure of the HA compound $[Ca_5(PO_4)_3OH]$, which were found in the following wavelength ranges: from 431-453 cm^{-1} (ν_2 vibrational mode); from 581-608 cm^{-1} (ν_4 vibrational mode); at 962 cm^{-1} (ν_1 vibrational mode); between 1028-1076 cm^{-1} (ν_3 vibrational mode) [33]. Fig.2b shows the spectrum for the active band of the OH^- group at 3574 cm^{-1} for the HA target, and at 3577 cm^{-1} for the HA-Si coating. Both the vibration of the hydroxyl group and the ν_1 mode of the phosphate group are distinctive of the HA phase and help to differentiate this compound from other calcium phosphates of similar molecular formula, but which have very different biological properties [34]. The results obtained evidence an adequate control in the deposition conditions of the multilayer coating.

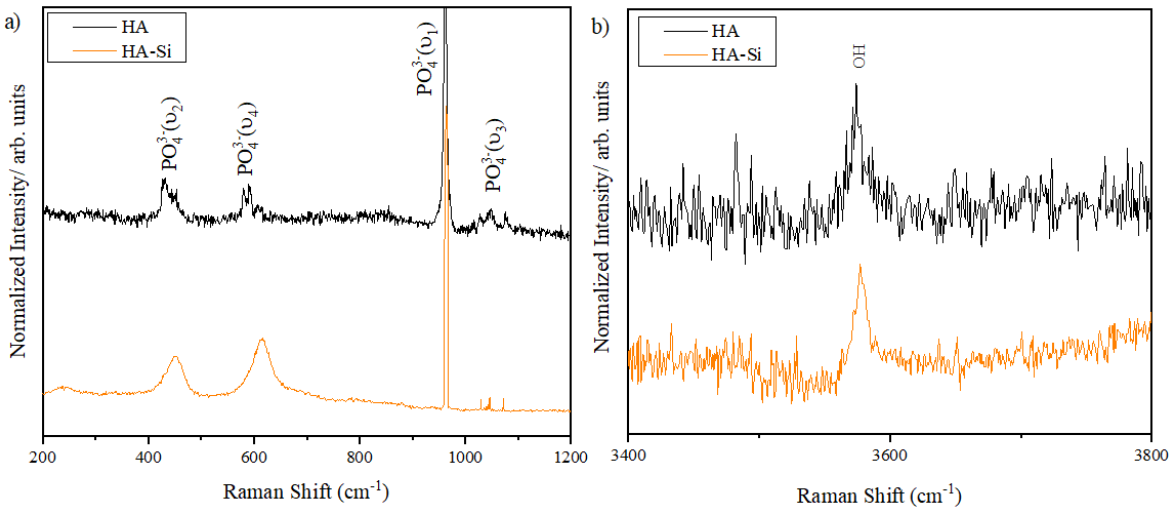

Fig. 2. Micro-Raman spectra for HA-Si multilayer coating and HA target:

a) 200-1200 cm^{-1}, b) 3400-3800 cm^{-1}.

3.2. Structure and roughness

Fig. 3 shows the SEM image of the cross-sectional structure of the HA-Si coating. It shows a dense and compact layer, which did not show evidence of a multilayer structure. However, it was observed by FESEM on a coating sample prepared by FIB, see Fig. 4. There, the multilayer structure of the HA-Si deposit on the Ti6Al4V substrate is evident, where the bonding between the multiple layers of the coating, and between these and the Ti6Al4V substrate, is observed. The coating is constituted by 5 HA layers, each approximately 55 nm thick, which are presented in the image with a light contrast; and 4 Si interlayers, each approximately 35 nm thick, which are presented in the image with a dark contrast. The total thickness of the multilayer coating was close to 415 nm. The architecture obtained in the multilayer coating is largely in accordance with the intended design. This type of structures allows the combination of properties between different compounds, which could enhance in this particular case, the biological response of the surface [35]. In addition, it has been found that the large number of interfaces in these multilayer systems, compared to monolayer coatings (with only 1 interface), can generate a relief of residual stresses due to a greater energy dissipation during the growth of the coating [28]. In addition, using multilayer systems it is possible to control the release of some elements to the medium and prolong its effect, in this case, the dissolution in biological medium of the HA, could generate the presence of Si ions at the surface level that favor the biological response of the coating.

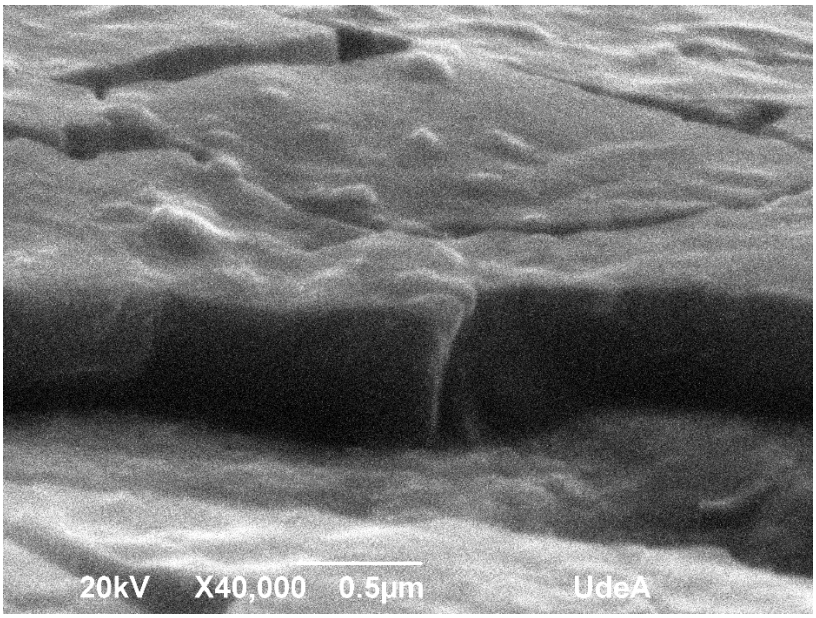

Fig. 3. Cross-section of HA-Si coating.

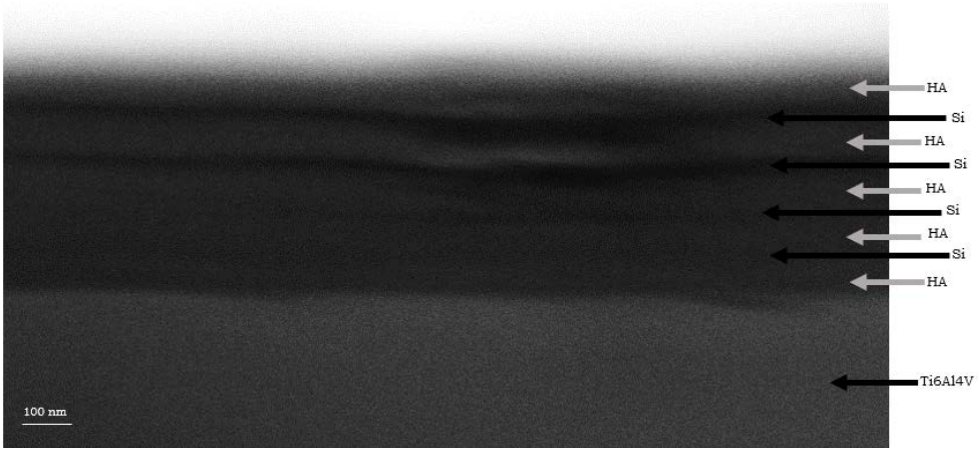

Fig. 4. FIB-FESEM cross-section at 63,000 X of the HA-Si/Ti6Al4V system.

Fig.5. shows the root-mean-square roughness values for the multilayer HA-Si coating as a function of the type of surface where it was deposited, Ti6Al4V (G) or (R). The interrupted horizontal lines present the roughness values obtained for these two conditions, which

correspond to 3.8 nm and 48.7 nm, respectively. On these surfaces, multilayer HA-Si coatings with roughness of 27.2 nm (smoother surface) and 52.5 nm (rougher surface) were grown. A hypothesis that could explain the behavior obtained is that, during the sputter deposition process, the atoms ejected from the target that reach the substrate surface grow on the substrate surface adopting a very similar profile, at least during the initial stages of the process, due to the close (atomic) contact level. All the above would indicate that the roughness characteristics in thin coatings can be controlled from the surface preparation of the substrates and thus obtain changes in the surface properties. It has been found that roughness influences the mechanical and biological properties of coatings [36], [37].

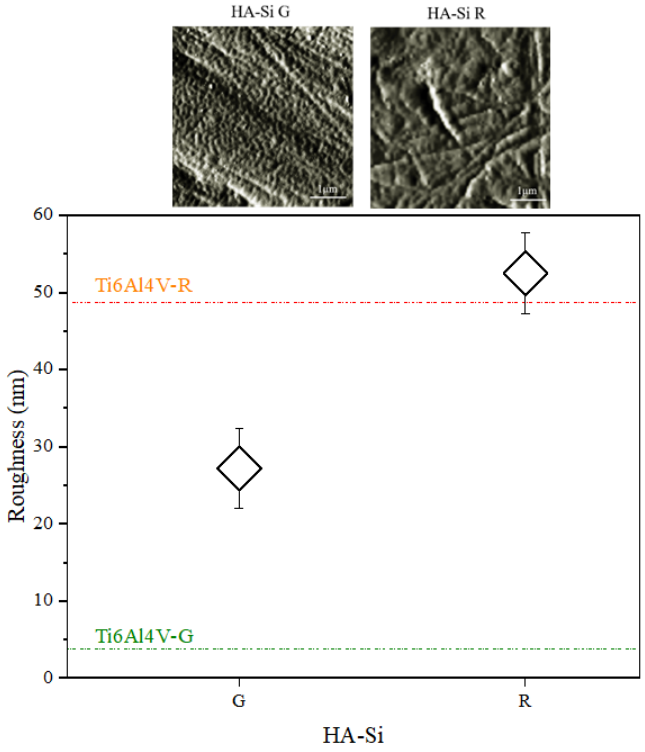

Fig. 5. Roughness of Ti6Al4V substrates with glass and rough preparation and their respective HA-Si coatings.

3.3. *In vitro* cell viability

Fig. 6 shows the results of the viability assay of mMSCs by MTT for the Ti6Al4V substrate (G) and the multilayer HA-Si coating deposited on it, compared to a glass control. There it is observed that cell viability increases from 94% on the Ti6Al4V substrate to approximately 107% on the HA-Si coating. Ti6Al4V alloy is widely used in the manufacture of implants due to its bioinert character, however, there is evidence of ion release when this metal is immersed in biological media: the Ti ion released does not significantly alter cell viability, but Al^{3+} and V^{2+} can be toxic and inhibit cell proliferation, with Al being implicated in diseases such as Alzheimer's, and V causing damage to respiratory and DNA chains structures [34]. Ion release has been reported to be present from the first hours of implantation, with high release peaks up to the third and fourth week [38]–[42]. As well as ion release from the substrate, Si ions from the multilayer coating can be released to the medium, as reported in an HA coating with Ag interlayers [43]. Considering all the above, the behavior obtained in the present study may indicate that the Si released through the HA layers favored the metabolic activity of the mMSCs promoting their viability. Fig.7 shows the morphology of the cells just before the start of the MTT assay. The number of cells in each system correlates with the viability percentages recorded.

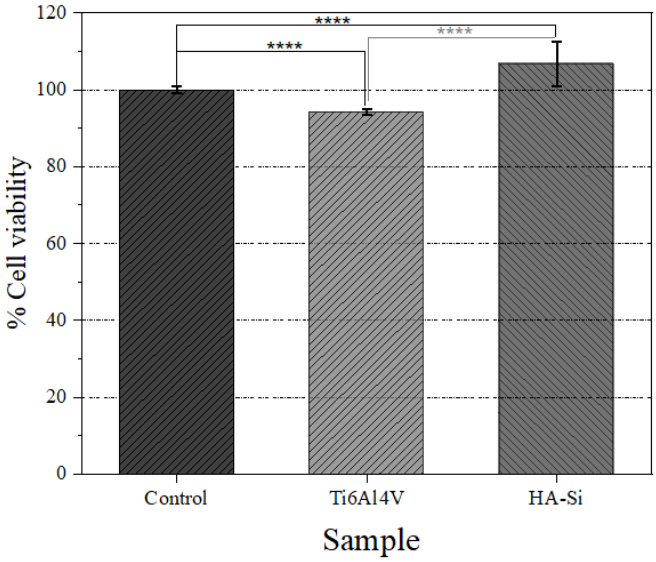

Fig. 6. Cell viability of Ti6Al4V substrate and HA-Si system on mMSCs. Significant values: ****p< 0.0001.

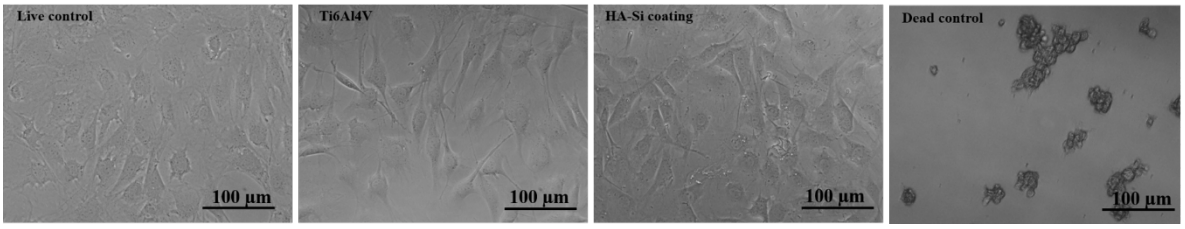

Fig. 7. Images of mMSCs after 72 hours.

3.4. Cell adhesion

Fig. 8 shows the mMSCs adhered on the substrate surface with different roughness levels (Ti6Al4V-G and Ti6Al4V-R) and the coatings deposited there (HA-Si-G and HA-Si-R), compared to a control. The fluorescent staining generated allowed us to observe both the morphology of the cell cytoskeleton (actin in red) and the focal adhesions of the cells on the surface of the substrate or coating (vinculin in green). Actin is a globular protein that forms

the microfilaments that conform the cytoskeleton, while vinculin evidences the focal adhesions that involve the anchoring of molecules to a surface. Fig. 8a shows the cells adhered on the substrate surface. There, it is evident that there was greater cell adhesion on the Ti6Al4V - R surface, since elongated cells are observed, compared to the Ti6Al4V - G system, where the cell morphology tends to be circular. This result evidence an effect of surface roughness on the cell anchoring process, since adhesion was higher on the rougher surface, which agrees with some literature reports, which indicate that cells undergo a change in their morphology and widen when they are on rough and hydrophilic surfaces [44], [45]. Additionally, a higher amount of focal adhesion zones is observed for cells seeded on the surface of Ti6Al4V - R. A similar behavior was recorded for HA-Si systems, where a more extended cell morphology is observed on the surface of the higher roughness coating (HA-Si - R), see Fig. 8b. Finally, Fig. 8c presents the adhesion of mMSCs on the control surface (glass). There, it is observed, as in Ti6Al4V - G system, a large circular trend in cell morphology and few areas of focal adhesion.

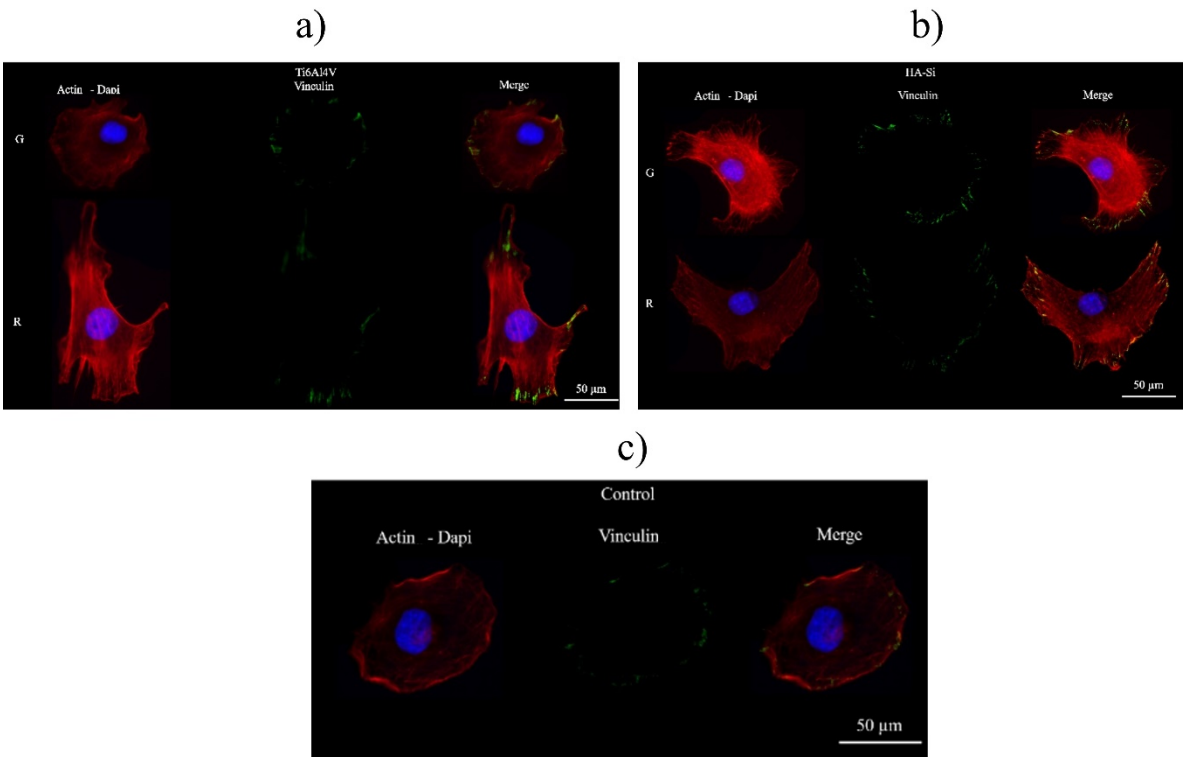

Fig. 8. Adhesion assay of mMSCs on the developed systems; cytoskeleton (Actin) in red; nucleus (Dapi) in blue; focal adhesions (Vinculin) in green.

To make quantitative comparisons between the cell adhesion results for the evaluated systems, Fig. 9 presents the graph of cell adhesion area and circularity. Fig. 9a shows that, for both systems studied (Ti6Al4V and HA-Si coating) there is an increase in the cell adhesion area when the surface roughness increases, obtaining statistically significant differences in both cases. However, in the HA-Si system, changes of greater magnitude were obtained in the average values in the expansion area, registering the highest value for the HA-Si - R coating. When comparing the results of the adhesion area considering the type of surface, it is observed that the Ti6Al4V - R and HA-Si - R samples present significant differences, indicating, in this case, a synergistic effect between surface roughness and

surface chemistry to obtain a better cell adhesion. In relation to the control used, cell expansion area was greater in the 4 samples evaluated. Fig. 9b presents the circularity values for the cells adhered to the different surfaces. A similar behavior to that of cell spreading described above: the circularity decreased as the surface roughness increased, indicating an improvement in the cell adhesion process, since the morphology presents elongated shapes. Considering the change in surface chemistry, a better behavior is observed in cells circularity when adhered on the HA-Si - R coating surface, compared to the Ti6Al4V - R system, evidencing again the favorable and complementary effect between the two evaluated characteristics, roughness and surface chemistry, this effect is also observed, but to a lesser extent, for the Ti6Al4V - G and HA-Si - G systems, where there are statistically significant differences in cell circularity when comparing the substrate and coating system.

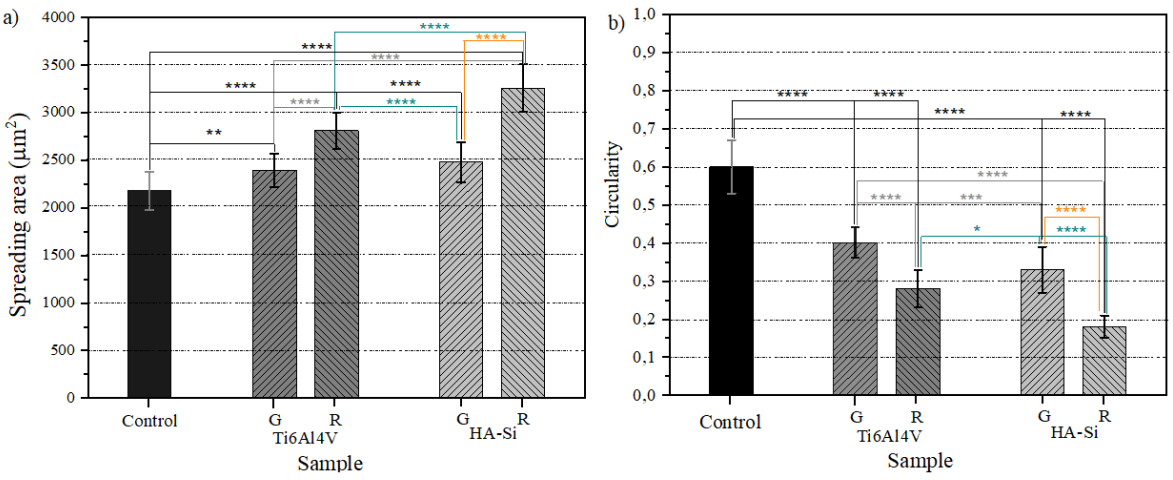

Fig. 9. a) Spreading area, b) circularity of mMSCs on Ti6Al4V substrate and HA-Si coating system. Significant values: ****p< 0.0001, ***p< 0.0005, **p= 0.0069, *p= 0.0127.

Fig. 10 presents the results of the focal adhesion area and focal adhesion number. The behavior shows that the area of focal adhesions increases when roughness is involved; compared to the control, it is found that the HA-Si coated substrates have the highest adhesion area, with the lowest adhesion area in Ti6Al4V - G, and the highest adhesion area in the HA-Si – R system. This pattern is repeated in Fig.10b corresponding to the number of focal adhesions, where the dominant system in focal adhesion number is the HA-Si - R coating.

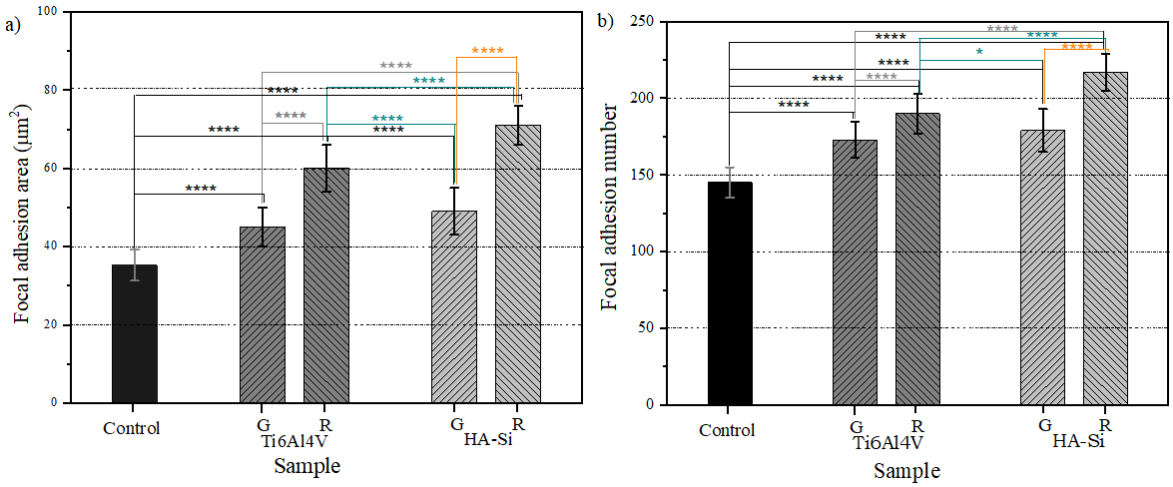

Fig. 10. (a) focal adhesion area, (b) focal adhesion number of mMSCs on Ti6Al4V substrate and HA-Si coating system. Significant values: ****p< 0.0001, *p= 0.0269.

The set of parameters previously analyzed shows that roughness as a surface characteristic affects the ability to allow cell adhesion and proliferation [46]. In addition, the presence of HA and Si modifies the interaction of the cytoskeleton and the adhesion of cells on the coating system. The success of implants at the biomedical level is determined by the interactions between the implant and the adjacent tissue. That is why the importance of the

multilayer coating on rough surface lies in the optimal values in expansion area, circularity, focal adhesion number and area, including that for this system the cell viability obtained the best results.

4. Conclusions

-HA phase in the coatings was confirmed by micro-Raman spectroscopic analysis, where characteristic vibrations of this compound, associated with the phosphate $(PO_4)^{-3}$ and hydroxyl (OH^-) functional groups, were registered

-The process parameters allowed to obtain HA-Si coatings with a Ca/P ratio of 1.66 and 1.73 atomic. % Si. Maintaining a multilayer structure confirmed by FIB-FESEM.

-The MTT assay indicates that the developed HA-Si coatings are potentially non-toxic.

-A synergistic effect between roughness and surface chemistry of a Ti6Al4V substrate on cell adhesion was found.

Acknowledgments

We thank the University of Antioquia, the Centro de Investigación, Innovación y Desarrollo de materiales (CIDEMAT) group, the Departamento Administrativo de Ciencia, Tecnología e Innovación (COLCIENCIAS) for financing the Project 15-1696, the scholarship program of Enlazamundos, the Agencia de Educación Superior de Medellín (Sapiencia), JLGR acknowledges financial support from the Spanish State Research Agency (AEI) through the PID2019-106099RB-C41 / AEI / 10.13039/501100011033 Project. PR acknowledges

support from the Spanish Ministry of Science, Innovation and Universities (RTI2018-096794), and Fondo Europeo de Desarrollo Regional (FEDER). CIBER-BBN is an initiative funded by the VI National R&D&I Plan 2008–2011, Iniciativa Ingenio 2010, Consolider Program. CIBER Actions are financed by the Instituto de Salud Carlos III with assistance from the European Regional Development Fund. The Microscopy Service of the UPV (Universitat Politècnica de València) is gratefully acknowledged for helping with FESEM characterization.

References

[1] L. Angarita, “Síntesis de películas delgadas por la técnica de magnetrón sputtering a partir de blancos de renio y boro,” *Tesis*, vol. 1, no. 1, pp. 11–92, 2017.

[2] A. H. Hamdy Makhlouf and I. Tiginyanu, *Nanocoatings and ultra-thin films*. 2011.

[3] R. A. Surmenev, “A review of plasma-assisted methods for calcium phosphate-based coatings fabrication,” *Surf. Coatings Technol.*, vol. 206, no. 8–9, pp. 2035–2056, 2012, doi: 10.1016/j.surfcoat.2011.11.002.

[4] E. Mohseni, E. Zalnezhad, and A. R. Bushroa, “Comparative investigation on the adhesion of hydroxyapatite coating on Ti-6Al-4V implant: A review paper,” *Int. J. Adhes. Adhes.*, vol. 48, pp. 238–257, 2014, doi: 10.1016/j.ijadhadh.2013.09.030.

[5] D. Brunette, P. Tengvall, M. Textor, and P. Thomsen, *Titanium in Medicine*, vol. 216, no. 3. 2002.

[6] F. Gil and J. Planell, “Aplicaciones biomédicas del titanio v sus aleaciones,”

Biomecánica, no. JANUARY 1993, pp. 34–42, 1993, [Online]. Available: http://upcommons.upc.edu/handle/2099/6814.

[7] C. F. Koch *et al.*, "Pulsed laser deposition of hydroxyapatite thin films," *Mater. Sci. Eng. C*, vol. 27, no. 3, pp. 484–494, 2007, doi: 10.1016/j.msec.2006.05.025.

[8] J. L. Ong, D. L. Carnes, and K. Bessho, "Evaluation of titanium plasma-sprayed and plasma-sprayed hydroxyapatite implants in vivo," *Biomaterials*, vol. 25, no. 19, pp. 4601–4606, 2004, doi: 10.1016/j.biomaterials.2003.11.053.

[9] M. A. Surmeneva *et al.*, "Preparation of a silicate-containing hydroxyapatite-based coating by magnetron sputtering: Structure and osteoblast-like MG63 cells in vitro study," *RSC Adv.*, vol. 3, no. 28, pp. 11240–11246, 2013, doi: 10.1039/c3ra40446c.

[10] S. Dorozhkin and M. Epple, "Biological and Medical Significance of Calcium Phosphates," *Angew. Chemie - Int. Ed.*, vol. 41, no. 17, pp. 3213–3215, 2002, doi: 10.1002/1521-3773(20020902)41.

[11] K. Ioku, M. Yoshimura, and S. Somiya, "Microstructure and mechanical properties of hydroxyapatite ceramics with zirconia dispersion prepared by post-sintering," *Biomaterials*, vol. 11, no. 1, pp. 57–61, 1990, doi: 10.1016/0142-9612(90)90053-S.

[12] H. Oonishi *et al.*, "Quantitative comparison of bone growth behavior in granules of Bioglass®, A-W glass-ceramic, and hydroxyapatite," *J. Biomed. Mater. Res.*, vol. 51, no. 1, pp. 37–46, 2000, doi: 10.1002/(SICI)1097-4636(200007)51:1<37::AID-JBM6>3.0.CO;2-T.

[13] O. Pereda Cardoso, R. Toca Caballero, and R. González Santos, "Resultados del relleno de defectos óseos tumorales con hidroxiapatita o injerto homólogo," *Rev.*

Cuba. Ortop. y Traumatol., vol. 20, no. 2, p. 0, 2006.

[14] R. A. Surmenev *et al.*, "Ab initio calculations and a scratch test study of RF-magnetron sputter deposited hydroxyapatite and silicon-containing hydroxyapatite coatings," *Surfaces and Interfaces*, vol. 21, no. August, p. 100727, 2020, doi: 10.1016/j.surfin.2020.100727.

[15] A. Vladescu *et al.*, "In vitro activity assays of sputtered HAp coatings with SiC addition in various simulated biological fluids," *Coatings*, vol. 9, no. 6, pp. 1–17, 2019, doi: 10.3390/COATINGS9060389.

[16] E. S. Thian, J. Huang, Z. H. Barber, S. M. Best, and W. Bonfield, "Surface modification of magnetron-sputtered hydroxyapatite thin films via silicon substitution for orthopaedic and dental applications," *Surf. Coatings Technol.*, vol. 205, no. 11, pp. 3472–3477, 2011, doi: 10.1016/j.surfcoat.2010.12.012.

[17] V. F. Pichugin *et al.*, "The preparation of calcium phosphate coatings on titanium and nickel-titanium by rf-magnetron-sputtered deposition: Composition, structure and micromechanical properties," *Surf. Coatings Technol.*, vol. 202, no. 16, pp. 3913–3920, 2008, doi: 10.1016/j.surfcoat.2008.01.038.

[18] Y. H. Jeong and H. C. Choe, "Electrochemical characteristics of cell cultured Ti-Nb-Zr alloys after nano-crystallized Si-HA coating," *J. Nanosci. Nanotechnol.*, vol. 15, no. 1, pp. 185–188, 2015, doi: 10.1166/jnn.2015.8385.

[19] Y. H. Jeong, H. C. Choe, and W. A. Brantley, "Hydroxyapatite-silicon film deposited on Ti–Nb–10Zr by electrochemical and magnetron sputtering method," *Thin Solid Films*, vol. 620, pp. 114–118, 2016, doi: 10.1016/j.tsf.2016.07.086.

[20] K. Szurkowska and J. Kolmas, “Hydroxyapatites enriched in silicon – Bioceramic materials for biomedical and pharmaceutical applications,” *Prog. Nat. Sci. Mater. Int.*, vol. 27, no. 4, pp. 401–409, 2017, doi: 10.1016/j.pnsc.2017.08.009.

[21] A. S. Andersson, F. Bäckhed, A. Von Euler, A. Richter-Dahlfors, D. Sutherland, and B. Kasemo, “Nanoscale features influence epithelial cell morphology and cytokine production,” *Biomaterials*, vol. 24, no. 20, pp. 3427–3436, 2003, doi: 10.1016/S0142-9612(03)00208-4.

[22] T. T. Paterlini, L. F. B. Nogueira, C. B. Tovani, M. A. E. Cruz, R. Derradi, and A. P. Ramos, “The role played by modified bioinspired surfaces in interfacial properties of biomaterials,” *Biophys. Rev.*, vol. 9, no. 5, pp. 683–698, 2017, doi: 10.1007/s12551-017-0306-2.

[23] M. Echeverry-Rendón, O. Galvis, R. Aguirre, S. Robledo, J. G. Castaño, and F. Echeverría, “Modification of titanium alloys surface properties by plasma electrolytic oxidation (PEO) and influence on biological response,” *J. Mater. Sci. Mater. Med.*, vol. 28, no. 11, Nov. 2017, doi: 10.1007/s10856-017-5972-x.

[24] A. M. Cazabat and M. A. C. Stuart, “Dynamics of wetting: Effects of surface roughness,” *J. Phys. Chem.*, vol. 90, no. 22, pp. 5845–5849, 1986, doi: 10.1021/j100280a075.

[25] R. N. Wenzel, “Resistance of solid surfaces to wetting by water,” *Ind. Eng. Chem.*, vol. 28, no. 8, pp. 988–994, 1936, doi: 10.1021/ie50320a024.

[26] S. Giljean, M. Bigerelle, K. Anselme, and H. Haidara, “New insights on contact angle/roughness dependence on high surface energy materials,” *Appl. Surf. Sci.*, vol.

257, no. 22, pp. 9631–9638, 2011, doi: 10.1016/j.apsusc.2011.06.088.

[27] J. A. Lenis, F. M. Hurtado, M. A. Gómez, and F. J. Bolívar, “Effect of thermal treatment on structure, phase and mechanical properties of hydroxyapatite thin films grown by RF magnetron sputtering,” *Thin Solid Films*, vol. 669, no. November 2018, pp. 571–578, 2019, doi: 10.1016/j.tsf.2018.11.045.

[28] J. A. Lenis, G. Bejarano, P. Rico, J. L. G. Ribelles, and F. J. Bolívar, “Development of multilayer Hydroxyapatite - Ag/TiN-Ti coatings deposited by radio frequency magnetron sputtering with potential application in the biomedical field,” *Surf. Coatings Technol.*, vol. 377, no. June, p. 124856, 2019, doi: 10.1016/j.surfcoat.2019.06.097.

[29] J. A. Lenis, P. Rico, J. L. G. Ribelles, M. A. Pacha-Olivenza, M. L. González-Martín, and F. J. Bolívar, “Structure, morphology, adhesion and in vitro biological evaluation of antibacterial multi-layer HA-Ag/SiO2/TiN/Ti coatings obtained by RF magnetron sputtering for biomedical applications,” *Mater. Sci. Eng. C*, vol. 116, no. July, p. 111268, 2020, doi: 10.1016/j.msec.2020.111268.

[30] M. Londoño López, A. Echevarría, and F. De La Calle, “Características cristaloquímicas de la hidroxiapatita sintética tratada a diferentes temperaturas,” *Rev. EIA*, no. 5, pp. 109–118, 2006.

[31] M. A. Surmeneva *et al.*, “Effect of silicate doping on the structure and mechanical properties of thin nanostructured RF magnetron sputter-deposited hydroxyapatite films,” *Surf. Coatings Technol.*, vol. 275, pp. 176–184, 2015, doi: 10.1016/j.surfcoat.2015.05.021.

[32] L. P. Alvarado Calderon, “Inducción del desarrollo reproductivo en Lactuca sativa, L., Var. Batavia larga, bajo las condiciones no inductivas de la sabana de bogotá,” p. 127, 2004.

[33] A. Sroka-Bartnicka *et al.*, “The biocompatibility of carbon hydroxyapatite/β-glucan composite for bone tissue engineering studied with Raman and FTIR spectroscopic imaging,” *Anal. Bioanal. Chem.*, vol. 407, no. 25, pp. 7775–7785, 2015, doi: 10.1007/s00216-015-8943-4.

[34] S. Duarte and Universidad Nacional de Asunción, “Síntesis y caracterización de fosfatos de calcio por el método sol-gel,” 2012.

[35] R. López, “Recubrimientos monocapa y multicapas funcionales, a base de Níquel, elaborados por técnicas de electrodepósito y de depósito químico dinámico (DCD),” 2013.

[36] M. González, R.; Vargas, F.; Esperanza, “Influence of the roughness in the microhardness and wear resistance of thermal spray coating,” *Sci. Tech. Año XIII*, no. 36, pp. 163–168, 2007.

[37] M. Vallet-Regí and J. M. González-Calbet, “Calcium phosphates as substitution of bone tissues,” *Prog. Solid State Chem.*, vol. 32, no. 1–2, pp. 1–31, 2004, doi: 10.1016/j.progsolidstchem.2004.07.001.

[38] T. Hanawa, “Metal ion release from metal implants,” *Mater. Sci. Eng. C*, vol. 24, no. 6-8 SPEC. ISS., pp. 745–752, 2004, doi: 10.1016/j.msec.2004.08.018.

[39] Y. Zhang *et al.*, “Effect of vanadium released from micro-arc oxidized porous Ti6Al4V on biocompatibility in orthopedic applications,” *Colloids Surfaces B*

Biointerfaces, vol. 169, no. May, pp. 366–374, 2018, doi: 10.1016/j.colsurfb.2018.05.044.

[40] M. Andrade, H. Estupiñan, D. Peña, and C. Vasquez, “Comportamiento electroquímico de aleación de Ti6Al4V anodizada en solución de NaH2PO4.2H2O,” *Sci. Tech.*, vol. XIII, no. 36, pp. 215–220, 2007, doi: 10.22517/23447214.4989.

[41] Y. Okazaki and E. Gotoh, “Comparison of metal release from various metallic biomaterials in vitro,” *Biomaterials*, vol. 26, no. 1, pp. 11–21, 2005, doi: 10.1016/j.biomaterials.2004.02.005.

[42] Y. Okazaki, S. Rao, S. Asao, T. Tateishi, S. Katsuda, and Y. Furuki, “Effects of Ti, Al and V Concentrations on Cell Viability,” *Mater. Trans.*, vol. 39, no. 10, pp. 1053–1062, 1998.

[43] J. A. Lenis, L. J. Toro, and F. J. Bolívar, “Multi-layer bactericidal silver - calcium phosphate coatings obtained by RF magnetron sputtering,” *Surf. Coatings Technol.*, vol. 367, no. March, pp. 203–211, 2019, doi: 10.1016/j.surfcoat.2019.03.038.

[44] S. A. Redey *et al.*, “Behavior of human osteoblastic cells on stoichiometric hydroxyapatite and type A carbonate apatite: Role of surface energy,” *J. Biomed. Mater. Res.*, vol. 50, no. 3, pp. 353–364, 2000, doi: 10.1002/(SICI)1097-4636(20000605)50:3<353::AID-JBM9>3.0.CO;2-C.

[45] S. Spriano *et al.*, “Surface properties and cell response of low metal ion release Ti-6Al-7Nb alloy after multi-step chemical and thermal treatments,” *Biomaterials*, vol. 26, no. 11, pp. 1219–1229, 2005, doi: 10.1016/j.biomaterials.2004.04.026.

[46] J. Gómez, L. E. Forero-Gómez, P. Escobar-Rivero, and W. Valdivieso, “Study of

cytotoxicity and adhesion of human osteosarcoma cells in superficially modified Ti6Al4V," *Sci. Tech.*, vol. 1, no. 36, 2007, [Online]. Available: http://revistas.utp.edu.co/index.php/revistaciencia/article/view/4933.